

MULTI-DOF ISOLATION AND ALIGNMENT WITH QUIET HYDRAULIC ACTUATORS

C Hardham³, B Abbott⁶, R Abbott⁶, G Allen³, R Bork¹, C Campbell³, K Carter⁶, D Coyne¹, D DeBra⁵, T Evans¹, J Faludi³, A Ganguli³, J Giaime⁴, M Hammond⁶, W Hua³, J Kern⁶, J LaCour⁶, B Lantz³, M Macinnis², K Maitland¹, K Mason², R Mittleman², J Nichol³, J Niekerk³, N Robertson³, D Ottaway², H Overmier⁶, J Phinney², B Rankin², D Sellers¹, P Sarin², D Shoemaker², O Spjeld⁶, G Traylor⁶, S Wen⁴, M Zucker⁶

¹ LIGO Laboratory, MS 18-34, California Institute of Technology, Pasadena, CA 91125, USA

² LIGO Laboratory, Bldg. NW17-161, Massachusetts Institute of Technology, Cambridge, MA 02139, USA

³ Ginzton Laboratory, Stanford University, Stanford, CA 94305, USA

⁴ Department of Physics and Astronomy, Louisiana State University, Baton Rouge, LA 70803, USA

⁵ Department of Aeronautics and Astronautics, Stanford University, Stanford, CA 94305, USA

⁶ LIGO Livingston Observatory, Box 940, Livingston, LA 70754, USA

1 INTRODUCTION

The goal of Advanced LIGO (Laser Interferometer Gravitational-Wave Observatory) is to detect gravitational waves. Detection is conducted by precisely monitoring the distance between reference mirrors with an interferometer. The perceived relative motion of the reference mirrors from gravitational waves is expected to be very small by comparison to seismic disturbances. A multi-stage isolation and alignment system is in development to hold the interferometer optics at their operating point and isolate them from external disturbances in all six degrees of freedom (DOF). While this problem is broadband, this paper focuses on the design of a unique actuator for a system which specifically addresses the low-frequency isolation and alignment requirements [1].

Based on predictions for low-frequency disturbances and other specifications of the total suspension [2], the requirements for the low-frequency system actuator are challenging. Four specifications define this challenge: max force greater than 2000 N; throw of ± 1 mm; bandwidth from zero frequency to at least 10 Hz; and noise not to exceed 10^{-9} m/ $\sqrt{\text{Hz}}$ at 1 Hz. While there are other actuators that meet one or more of these requirements, the ‘Quiet Hydraulic’ actuator is one known solution which can meet all of these requirements without the nonlinear, stick-slip behavior typical of mechanical solutions or appreciable hysteresis.

1.1 QUIET HYDRAULICS

Quiet hydraulics differs principally from conventional hydraulics in that the flow in the system is not permitted to become turbulent. By maintaining laminar flow through-

out the system, a quiet hydraulic actuator can reach very low noise levels.

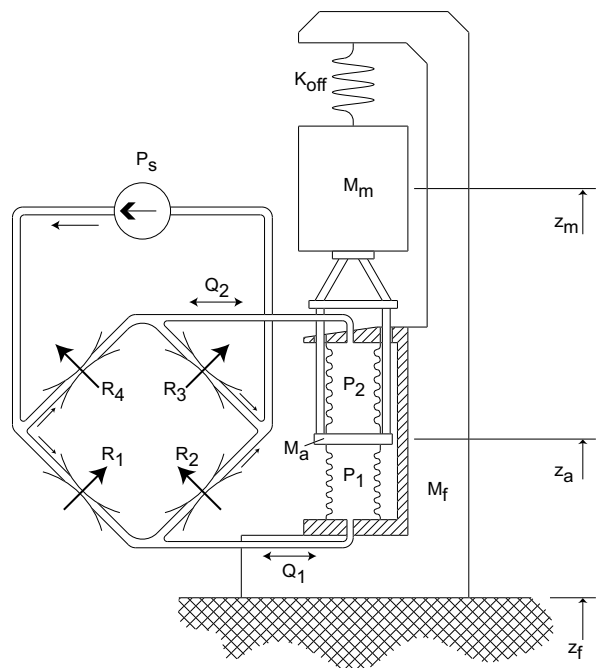


Figure 1: The actuator is comprised of five principle parts. The pump, P_s , provides constant volumetric flow. The flow is then sent through a servo valve that contains the hydraulic equivalent of a Wheatstone bridge with variable resistances R_1, R_2, R_3 and R_4 that are controlled in differential pairs. By controlling the position of the flappers in the servo valve, the pressure at the intermediate nodes of the bridge, P_1 and P_2 , are changed thereby modifying the flow, Q_1 and Q_2 , to the bellows. The differential

pressure created at the intermediate nodes of the bridge is applied to the actuator plate, M_a , by the area enclosed by the bellows thus creating force.

A schematic diagram for the quiet hydraulic actuator with a suspended load is shown in Figure 1. The piston of the actuator is comprised of an actuator plate, M_a , between two flexible bellows. By using flexible elements to construct the piston chambers, all frictional interfaces typical of conventional hydraulic seals are avoided.

2 THE HYDRAULIC SERVO VALVE

The purpose of the hydraulic flapper valve, or servo valve, is to provide control of differential pressure in the bellows of the actuator.

The servo valve used in this experiment (a modified Parker DYP-2S) contains two electro-magnetically controlled flappers and four nozzles (Figure 2). Each flapper, and the associated pair of nozzles, represents two differentially controlled variable resistances, or one-half of the bridge shown in Figure 1 (i.e. R_1 and R_2 or R_3 and R_4). The flappers are controlled such that they move in opposite directions. If the valve is tuned properly, this means that $R_1 = R_3$ and $R_2 = R_4$.

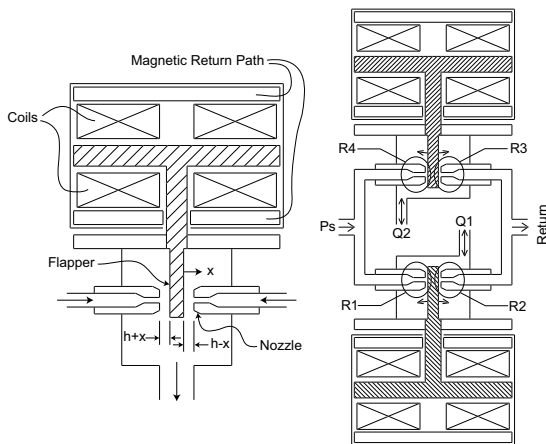


Figure 2: The active components of a flapper valve (left) and the Parker DYP-2S valve (right)

The variable resistance of the flapper valve is controlled by current inputs to the coil. In response to the control current, the flapper rotates in x , reducing the gap, $h - x$, between the flapper and nozzle on one side (greater hydraulic resistance), while increasing the gap, $h + x$, on the opposite side (smaller hydraulic resistance).

2.1 THE NOZZLE - FLAPPER RESISTANCE

The hydraulic resistance of the nozzle - flapper combination is comprised of two resistances: the variable resistance created by the gap between the nozzle face and the flapper, and the fixed resistance of the nozzle.

The variable resistance can be approximated by a parallel plate impedance which has a cubic dependance on the distance, $h \pm x$ (Figure 2), between the flapper and the nozzle.

$$R_{flapper} = R_o \cdot \left(\frac{1}{1 \pm \epsilon} \right)^3 \quad (1)$$

$$R_o = \frac{12\mu}{2\pi h_{avg}^3} \cdot \log \left(\frac{r_o}{r_i} \right) \quad (2)$$

Here, h_{avg} is the nominal, flapper centered, gap; r_i and r_o are the inner and outer diameters of the nozzle face; μ is the viscosity; and $\epsilon = x/h$. The total resistance of a nozzle - flapper combination is:

$$R = R_n + R_o \left(\frac{1}{1 \pm \epsilon} \right)^3 \quad (3)$$

where R_n is the nozzle resistance.

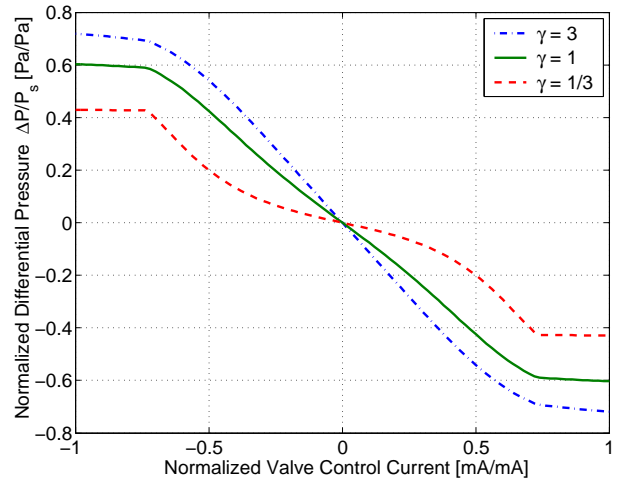


Figure 3: Normalized differential pressure as a function of normalized valve control current. $\gamma = R_o/R_n$

2.2 NOZZLE DESIGN

In its stock configuration, there are two important shortcomings of the nozzle - flapper configuration that must be mitigated before the valve can be used for this experiment. First, the sharp edges must be removed from the nozzles such that turbulence does not occur. This is easily remedied by thickening the edge of the nozzle orifice. The second issue is that the cubic dependance on flapper position yields a non-linear response which is undesirable for control.

Fortunately, it is possible to linearize the dependance of resistance on flapper position by carefully choosing the value of the fixed nozzle resistance, R_n [3]. The idea is to choose R_n such that it dominates the total resistance at large flapper displacements. The result of this approach is illustrated in Figure 3.

3 MATHEMATICAL MODELS

Several one dimensional models have been developed to explain the essential behavior of the hydraulic actuator. With a linearized expression for the servo valve, the basic equations of motion for the actuator are (see Figure 1):

$$(M_m + M_a)\ddot{z}_a = \Delta P A_b + K_{off}(z_g - z_a) + D \quad (4)$$

$$\Delta \dot{P} = \frac{2\beta}{V_b} \left(A_b(z_g - z_a) - \frac{\Delta P}{R_o} - \frac{P_S \epsilon}{R_o} \right) \quad (5)$$

where D is the seismic disturbance, ΔP is the differential pressure, β is the bulk modulus of the fluid, V_b is the bellows volume, and A_b is the area of the bellows.

4 ACTUATOR DEVELOPMENT

4.1 ACTUATOR DESIGN

The foundation of quiet hydraulic design is the complete omission of friction and rolling interfaces. At the core of this philosophy is the stacked bellows that are the quiet hydraulic piston (Figure 1). In addition to the bellows, there are parallel motion flexures and a tripod flexure that enable this piston design to operate in multi-DOF systems (Figure 4).

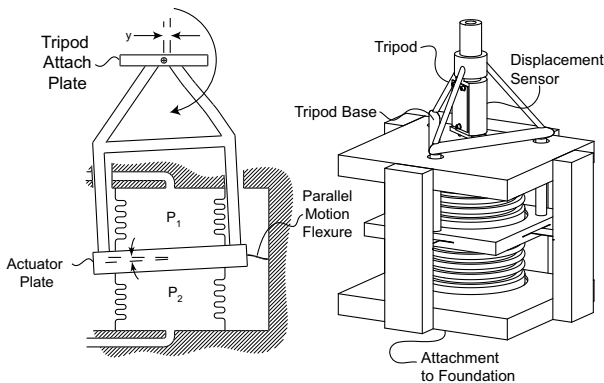


Figure 4: (1) (Left) Transverse motions, y , are accommodated by a tilting of the actuator plate and a rotation of the actuator attach plate. (2) (Right) The first prototype actuator.

Nominally, the parallel motion flexures guide the actuator plate in the direction of actuation. However, when the actuator is implemented in a multi-DOF system, the parallel motion flexures are used in combination with the tripod flexure to accommodate transverse motions. To this end, the tripod flexure is designed to be soft in rotations while stiff along the axis of actuation. When the tripod attach plate is translated off-axis, the actuator plate must tilt because of the parallel motion flexures (Figure 4). This tilt is absorbed by the tripod, but since there is a considerable distance between the tripod base and the actuator plate, the tripod attach plate ends up in a translated position.

4.2 TEST PLATFORM

A platform was constructed to test the actuator. In an attempt to best match the final system, the test platform orients two actuators orthogonally (horizontal and vertical) around a suspended mass that mimics the mass for one corner of the final system. The test platform, and the initial prototype (Figure 4), were used to demonstrate the isolation and alignment performance specifications set forth in the introduction.

5 HYDRAULIC RESONANCE

Figure 5 compares the model from section 3 to data gathered from the vertical actuator on the test platform. The prominent spike in the data is caused by a hydraulic resonance that is much lower than originally expected. The model can reproduce the data, with reasonable fidelity, when the bulk modulus is set to be almost three orders of magnitude lower than expected (even accounting for air entrapment). In reality, the cause of the reduced resonant frequency is the *breathing stiffness* of the bellows. Breathing stiffness refers to the ability of a bellow to maintain a constant volume while the internal pressure is varied and the ends of the bellows are held fixed.

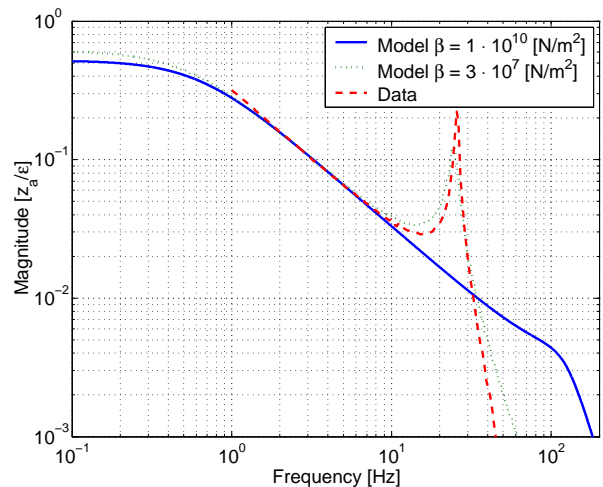


Figure 5: Driven transfer function of valve drive, ϵ , to actuator plate position, z_a , measured by the displacement sensor. The model is shown for two values of bulk modulus, β , and compared to data.

The resonance shown in Figure 5 does not render the system uncontrollable. Indeed, performance exceeding the LIGO specification has been demonstrated while this peak was digitally inverted, but for long-term operation, such as in the final implementation at the LIGO site, stability and robustness are essential. Therefore, two approaches were considered to passively mitigate this problem: redesign of the bellows and the addition of a bypass network.

5.1 BELLOW DESIGN

A successful bellow design must maximize the breathing stiffness while maintaining axial compliance. This is to avoid wasting a large percentage of the overall force generated in the actuator displacing the bellows. The searchable space to optimize the ratio of breathing stiffness to axial stiffness includes the diameter of the bellow, the thickness, and the convolution geometry.

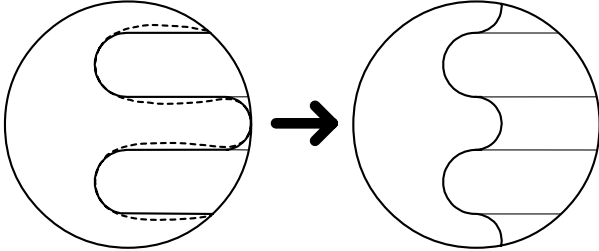


Figure 6: Close up details of the original bellows (left) and the new bellows (right). The dashed segments on the original design represent the distorted shape predicted by FE analysis of a 100 *psi* internal load.

The convolution geometry of the original bellow (Figure 6) performed poorly due to flat sections in the convolutions. Omitting the flats does improve the breathing stiffness, but at the cost of increased axial stiffness. The axial stiffness can be decreased by decreasing the thickness or increasing the length, but both of these choices reduce the breathing stiffness.

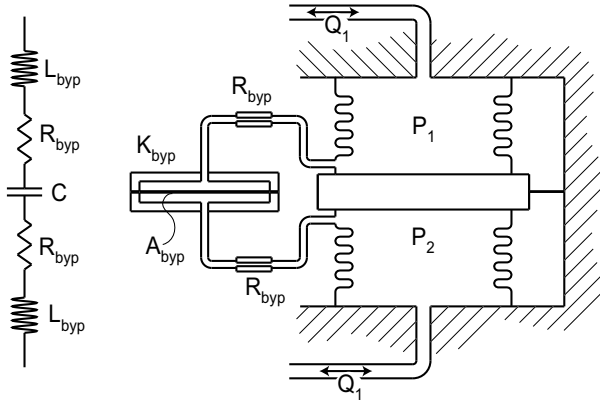


Figure 7: An electrical and schematic representation of the bypass network.

In order to determine the optimum combination of convolution geometry, wall thickness and length, several numerical approaches were adopted along with analytical solutions when available. Based on this search the breathing stiffness was improved from $1.70 \cdot 10^7$ N/m to $8.50 \cdot 10^7$ N/m with only a small increase in axial stiffness. Unfortunately, it has been difficult to experimentally validate this improvement, and to some extent, capitalize on this because the foundation that supports the actuator has a stiffness that is comparable, or less than, the original breathing stiffness.

5.2 THE BYPASS NETWORK

The search for a stiffer bellow revealed that it is difficult to attain the level of stiffness required to significantly increase the frequency of the bellows breathing resonance. An alternative approach is to passively damp the resonance with the addition of a bypass network.

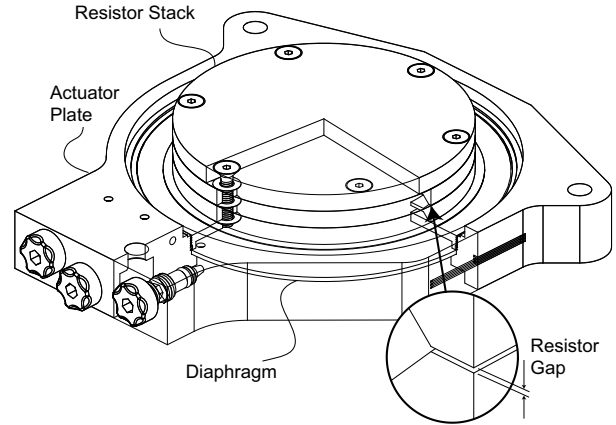


Figure 8: The resistor stack on the integrated to the actuator plate.

The bypass network is the hydraulic analog of a resistor and capacitor set in series between the two bellows (Figure 7). The hydraulic RC network is comprised of a flexible diaphragm as a capacitor and a flow constriction for a resistance. The resistance of is set to $1/25$ the bridge resistance and the diaphragm stiffness is set so that the pole is at 8 Hz which is low enough to damp the undesirable resonance but not deteriorate the authority of the actuator. However, care must be taken in the design of the resistance because, due to inductance, the impedance of the path leading to the diaphragm can be large enough to render the bypass useless.

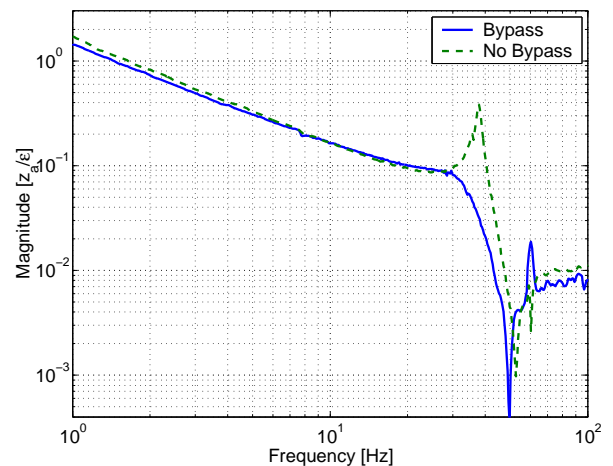


Figure 9: Suppression of hydraulic resonance with bypass network.

The pursuit of a relatively to provide good damping in combination with a very low inductance led to a parallel plate configuration with a small gap spread over a large width. This solution is efficiently packaged by spreading the width out over the perimeter of several rings stacked on top of each other (Figure 8). The resulting inductance is less than 1/100 of the resistance at 30 Hz.

6 FINAL ACTUATOR DESIGN

The final actuator design incorporates the improved bellows design and the bypass network. This actuator also features an internal bleed network operated by six pin valves (beneath the round, knurled caps), and an updated tripod that is axially stiffer while maintaining the rotational softness by the addition of the notches highlighted in Figure 10.

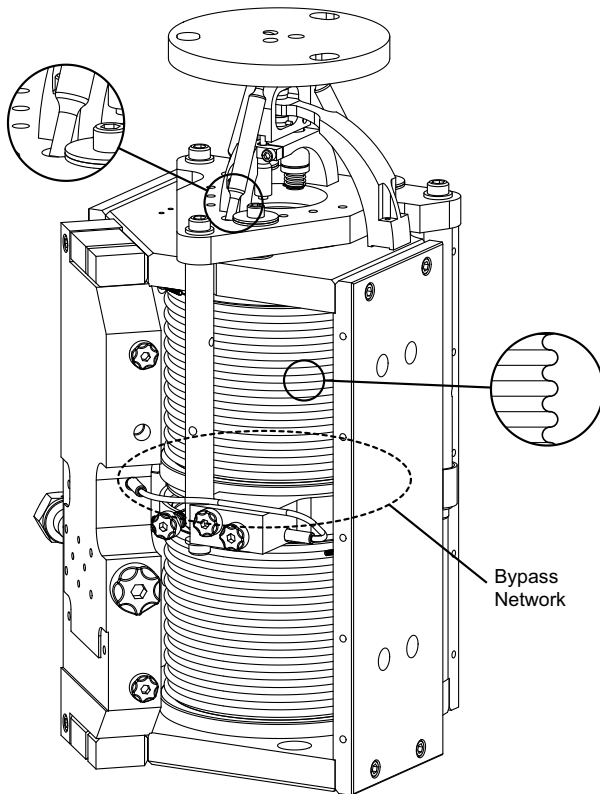


Figure 10: The third and final hydraulic actuator prototype.

7 CONTROL SCHEMES

The performance requirements for the LIGO application include both alignment and isolation. The alignment specification requires displacement feedback at low frequencies. Conversely, isolation requires inertial information used in either feedforward or feedback. In order to achieve both of these somewhat conflicting goals, two less conventional controls techniques are applied: sensor blending and sensor correction.

7.1 SENSOR BLENDING

Sensor blending is the combination of two sensor outputs. It is typically applied when information is desired over a broad range of frequencies but available sensing schemes are limited to specific bands of frequency. In this experiment, this approach is used to blend the displacement sensor and the feedback seismometer together into a *supersensor*. When the supersensor is used in feedback, it is possible to control position at low frequency while still attaining isolation at higher frequencies.

7.2 SENSOR CORRECTION

Sensor correction is defined here as the subtraction of undesired signal from a sensor output. In this experiment the displacement sensor measures the difference between the actuator plate position, z_a , and the ground/foundation position, z_f . A feedback loop operating to null the output of the displacement sensor will force $z_a = z_f$. This is directly at odds with the goal of isolation, and hence, the ground motion z_f is said to contaminate the displacement sensor output. Sensor correction is applied here by measuring the ground/foundation position explicitly with a low-frequency seismometer. This signal can be added to the displacement sensor output to cancel a large portion of the z_f term enabling the displacement sensor feedback to null the actuator plate position z_a and provide isolation.

8 QUIET HYDRAULICS IN LIGO

The final implementation in LIGO entails multiple installations around two different payload configurations designated: the BSC and the HAM. Both the BSC and the HAM payloads are constructed around four points of support requiring an eight actuator installation to control six DOF. At each support point there is a vertical and a tangentially oriented horizontal actuator. Each actuator is outfitted with a displacement sensor (Kaman DIT 5200) and a passive 1 Hz seismometer (Sercel L4C) for feedback control, and each group of eight actuators may reference a ground based, 3-axis, active seismometer (Streckheisen STS2) for sensor correction.

8.1 CONTROL STRATEGIES

A modal decomposition is applied to the signals from the eight feedback sensor pairs and the control signals to the actuators. The basis used was x, y, z, R_x, R_y and R_z with two additional over-constrained modes: OC_H and OC_V . This basis was chosen in consideration of the LIGO requirements which are prescribed for displacements in x, y and z .

For the x, y and z modes, the displacement sensor output is corrected using the inertial information from

the ground based seismometer. In these principle directions, the corrected displacement sensor output is blended with the feedback inertial sensors to make modal supersensors. Simple lead-lag controllers are applied to these modal supersensors to achieve upper unity gain crossovers of approximately 20 Hz and feedback gains approaching 100 at 1 Hz.

In the rotational modes, simple displacement feedback control is applied to minimize platform tilt. The over-constrained modes are also controlled with displacement feedback control to suppress noise sources (e.g. pump pressure fluctuations).

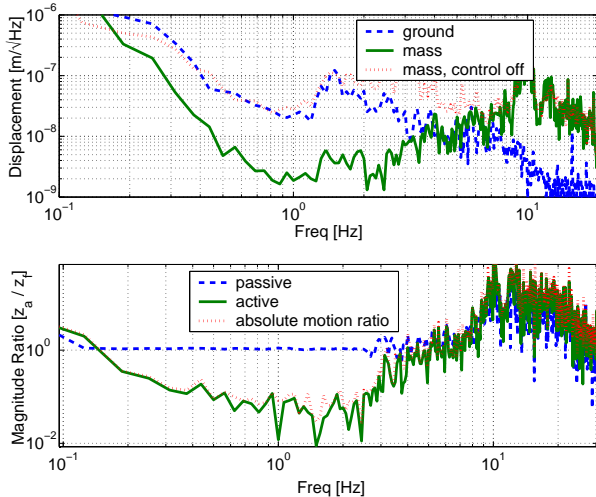


Figure 11: Isolation performance in the x direction for the BSC installation. Note that the ground motion at LASTI is much larger than at the LIGO sites. Upper plot: amplitude spectral density of motion, and lower, transmission ratio.

8.2 RESULTS

Early in 2004, LIGO began installing quiet hydraulic actuators in the Livingston observatory [4]. Prior to this, the quiet hydraulic actuators were installed and tested on a BSC at the LIGO Advanced System Test Interferometer (LASTI) facility at MIT.

Many of the control strategies discussed in section 8.1 were applied in this installation. However, there were two major sources of unexpected structural compliance that compromised some of the control algorithms and the resulting performance. The first difficulty arose from compliance between the horizontal actuators and the feedback seismometers. This rendered the horizontal seismometers unsuitable for feedback purposes. Hence, the isolation

performance in the horizontal directions is derived entirely from sensor correction and is not as good as anticipated at frequencies above 3 Hz (Figure 11).

The floor at LASTI was also more compliant than expected. As a result the sensor correction loop could, at times, become unstable due to interaction between the payload and the ground based seismometer. This results from the horizontal translation of the payload deforming the floor and causing the ground based seismometer to tilt. The seismometer measures tilt as horizontal motion which is then injected into displacement feedback error signal causing the platform to accentuate the problem. This limited the low frequency isolation performance of the horizontal directions.

9 CONCLUSIONS

A quiet hydraulic actuator has been developed for use in LIGO. This evolved actuator features a variety of improvements including a novel approach to damping of undesirable modes. This actuator has been implemented in an eight actuator, six DOF platform where low-frequency isolation performance has been demonstrated in the translational directions.

Installation of the quiet hydraulic actuators is underway at LIGO Livingston observatory. Performance at the Livingston observatory is expected to be improved by a much stiffer floor and improved collocation of the feedback seismometers.

References

- [1] Abramovici et. al., "LIGO - The Laser Interferometer Gravitational-wave Observatory," *Science*, 256, (1992), pp. 325-333.
- [2] D. Shoemaker, D. Coyne, "LIGO II Seismic Isolation Design Requirements Document," LIGO internal document LIGO-E990303-02-D, Nov 4, 1999, <http://www.ligo.caltech.edu/docs/E/E990303-02.pdf>.
- [3] Wu, Hsueh-Chieh. *Ultra-Precision Carriage Positioning of a Quiet Hydraulic Test Bed* Stanford: Stanford University, November 2000.
- [4] R. Abbott et. al., "Seismic Isolation Enhancements for Initial and Advanced LIGO," *Classical and Quantum Gravity*, volume 21, issue 5, pages S915 - S921.